

# Co-ordination of weak field ligands by *N*-acetylmicroperoxidase-8 (NAcMP8), a ferric haempeptide from cytochrome *c*, and the influence of the axial ligand on the reduction potential of complexes of NAcMP8 †

Helder M. Marques,<sup>\*a</sup> Ignacy Cukrowski<sup>b</sup> and Preeti R. Vashi<sup>a</sup>

<sup>a</sup> Centre for Molecular Design, Department of Chemistry, University of the Witwatersrand, Johannesburg, 2050 South Africa. E-mail: hmarques@aurum.chem.wits.ac.za

<sup>b</sup> Applied Chemistry and Chemical Technology Centre, Department of Chemistry, University of the Witwatersrand, Johannesburg, 2050 South Africa

Received 24th December 1999, Accepted 17th February 2000

Published on the Web 3rd April 2000

*N*-Acetylmicroperoxidase-8 (NAcMP8), a ferric haempeptide derived from cytochrome *c*, retains the His-18 ligand and, in addition, has a readily-displaced coordinated water molecule. The co-ordination of ligands which leave Fe(III) in a predominantly high spin state has been investigated by difference UV–visible spectrophotometry. The affinity for these ligands is low ( $K = 0.69, 0.45, 0.46$  and  $0.35 \text{ dm}^3 \text{ mol}^{-1}$  for co-ordination of  $\text{Cl}^-$ ,  $\text{Br}^-$ ,  $\text{I}^-$  and  $\text{SCN}^-$ , respectively), and somewhat larger for  $\text{N}_3^-$  ( $K = 25 \text{ dm}^3 \text{ mol}^{-1}$ ), where the metal is in an equilibrium between an admixed spin state ( $S = 3/2, 5/2$ ) and a low spin state ( $S = 1/2$ ). By contrast, previous work has shown that the affinity of Fe(III) for ligands that produce a low spin state is considerably larger ( $K = 10^2$  to  $>10^6 \text{ dm}^3 \text{ mol}^{-1}$ ). The effect of the axial ligand on the potential of the Fe(III)/Fe(II) couple in complexes of L–NAcMP8 (L = ligand *trans* to His-18) in aqueous solution at a glassy carbon electrode has been examined by cyclic voltammetry. The potentials of the quasi-reversible reduction of the halo complexes of NAcMP8 decrease in the order  $\text{L} = \text{Cl}^- > \text{Br}^- > \text{I}^-$  and reflect the hardness of the coordinated anion. The reduction potentials of some low spin complexes investigated (L = imidazole, ethanolamine, glycine, propylamine, cyanide) span less than 50 mV ( $E_2 = -0.203 \pm 0.015 \text{ V}$  vs. NHE), and are similar to complexes in which the metal is in a spin equilibrium (L =  $\text{OH}^-$ ,  $\text{N}_3^-$ ;  $E_2 = -0.209 \pm 0.005 \text{ V}$ ), whereas high spin complexes (L =  $\text{H}_2\text{O}$ ,  $\text{Cl}^-$ ,  $\text{Br}^-$ ,  $\text{I}^-$ ,  $\text{SCN}^-$ ) have somewhat higher reduction potentials ( $E_2 = -0.146 \pm 0.023 \text{ V}$ ). Work with pyridine and primary amine ligands shows that an increase in ligand basicity stabilises the Fe(III) state relative to the Fe(II). The rate constants for heterogeneous electron transfer are relatively insensitive to the nature of the axial ligand. Thus, changing the axial ligand of an iron porphyrin modulates the reduction potential only by a relatively small amount. The implications of this observation for biological systems is discussed.

## 1 Introduction

Peptic and tryptic digestion of cytochrome *c* produces the haemopeptide known as microperoxidase-8 (MP8 ‡, Fig. 1).<sup>1,2</sup> It retains the His residue as proximal ligand, contains bound  $\text{H}_2\text{O}$  in the other axial position, and provides a realistic model for the active site of haemoproteins that contain a single His as an axial ligand for iron.<sup>3,4</sup> Like many iron porphyrins, MP8 is monomeric only at low concentrations in aqueous solution.<sup>5</sup> Since only sub-micromolar concentrations are required in catalytic studies, the compound has been used successfully as a model for the peroxidase enzymes<sup>6–11</sup> and cytochrome P450.<sup>12</sup> Many physical and spectroscopic studies of MP8 require significantly higher concentrations. Aggregation by inter-

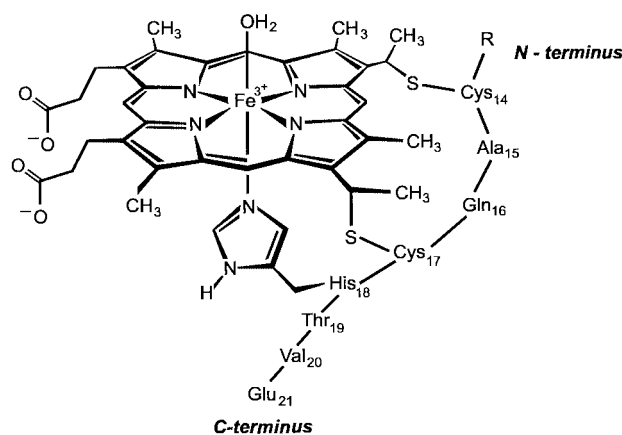


**Fig. 1** The haemopeptide microperoxidase-8 (MP8,  $\text{R} = \text{NH}_3^+$ ) obtained by the peptic and tryptic digestion of cytochrome *c*. The numbering of the amino acid residues is that of the parent protein. Acetylation of the *N*-terminal amino group ( $\text{R} = \text{NHCOCH}_3$ ) to produce *N*-acetylmicroperoxidase-8 (NAcMP8) significantly reduces the propensity of this species to undergo oligomerisation in solution. A number of related haemopeptides (MP11, MP9, MP6) have been prepared and studied (ref. 3).

molecular co-ordination through the *N*-terminal amino group of the peptide, and  $\pi$ – $\pi$  interaction, leads to the formation of low spin dimers and higher aggregates,<sup>5,13</sup> complicating the

† Electronic supplementary information (ESI) available: equilibrium constants for co-ordination of various ligands to haempeptides and plots of peak cathodic current against scan rate for NAcMP8. See <http://www.rsc.org/suppdata/dt/b0/b000065p/>

‡ Abbreviations used: CAPS, 3-(cyclohexylamino)-1-propanesulfonic acid; CHES, 2-(*N*-cyclohexylamino)ethanesulfonic acid; FePIX, iron-protoporphyrin IX; MOPS, 3-(*N*-morpholino)propanesulfonic acid; MPX, the haempeptide from cytochrome *c* where X is the number of amino acid residues from the original protein retained in the haempeptide; OEP, the dianion of octaethylporphyrin; TPP, the dianion of  $\alpha, \beta, \delta, \gamma$ -tetraphenylporphine; (2,6-F<sub>2</sub>)TPP, the dianion of  $\alpha, \beta, \delta, \gamma$ -(2,6-difluoro)tetraphenylporphine; UHF/SCF, unrestricted Hartree–Fock/Self Consistent Field;  $\mu$ , ionic strength ( $\text{mol dm}^{-3}$ ).

interpretation of the results. Acetylation of the *N*-terminus to produce *N*-acetylmicroperoxidase-8 (NACMP8) significantly decreases aggregation and a thorough characterisation<sup>14</sup> and an investigation of the behaviour of this species in aqueous solution<sup>15</sup> have been reported.

The co-ordinated H<sub>2</sub>O molecule is readily replaced by a variety of exogenous ligands.<sup>3,16</sup> This affords the possibility of systematically examining the effect a single axial ligand has on the properties of an iron porphyrin. We have previously compared and contrasted the kinetics<sup>17,18</sup> and thermodynamics<sup>3,16</sup> of the replacement of co-ordinated H<sub>2</sub>O (in NACMP8 in aqueous solution, or in MP8 in 20% MeOH) with data for the haemoproteins; we now consider the influence the axial ligand has on the potential of the Fe(III)|Fe(II) couple.

A number of groups have reported on the direct electrochemistry of haempeptides in aqueous or non-aqueous solution. Cyclic voltammetry was used to study the diffusion-controlled electron transfer to the haem undecapeptide, MP11, at a glassy carbon electrode<sup>19</sup> and at a silver electrode<sup>20</sup> in aqueous solution. It is likely<sup>21</sup> that MP11 was present as dimers or higher aggregates. Detergents above their critical micellar concentration have been used to address the aggregation problem.<sup>22</sup> The reduction potential,  $E_3$ , is slightly dependent on the identity of the detergent, but does not differ by more than 50 mV from that observed in aqueous solution; thus, the state of aggregation of a haempeptide has only a minor effect on the observed reduction potential. Some studies have explored the influence of the axial ligand on the electron transfer process. The rate of the chemical reduction of MP11 and MP9 by dithionite is independent of the axial ligands of Fe(III),<sup>23,24</sup> as is the self-exchange rate constant for MP8.<sup>25</sup> The addition of histidine to an aqueous solution of MP11<sup>20</sup> causes the reduction potential to shift negatively by some 40 mV at a silver electrode. Two anodic waves were observed; the peak current of one varied linearly with the scan rate, indicative of absorption of MP11 onto the electrode surface.

To further explore the co-ordination chemistry of the MPs, we report on the co-ordination of NACMP8 by some weak field ligands; we then focus attention on what effect the identity of the axial ligand has on the reduction potential of the Fe(III)|Fe(II) couple in NACMP8 in aqueous solution.

## 2 Experimental

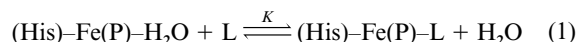
### 2.1 Materials and instrumentation

UV-visible spectra were recorded on a Cary 1 or a Cary 3 spectrophotometer with the cell compartment thermostatted with a water-circulating bath (25.0 ± 0.2 °C). Cyclic voltammetry (CV) was performed using an Autolab PGSTAT10 potentiostat (EcoChemie B.V., Netherlands) and controlled by GPES (General Purpose Electrochemical Systems, GPES AUTOLAB software, v. 4.5, EcoChemie B.V., P.O. Box 85163, 3508 AD Utrecht, The Netherlands, 1997) version 4.5 software. The scan rate was varied between 10 and 1000 mV s<sup>-1</sup>. A 5 mm diameter glassy carbon electrode was used as the working electrode. The electrode surface was prepared on a regular basis by polishing it with 6 micron diamond paste followed by sonication. Ag|AgCl was used as the reference electrode and a Pt wire as the auxiliary electrode. All CV experiments were performed on 2 cm<sup>3</sup> of a 9.89 × 10<sup>-4</sup> mol dm<sup>-3</sup> solution of NACMP8 in the presence of the appropriate ligand under an N<sub>2</sub> atmosphere in a thermostatted cell (25.0 ± 0.2 °C). In all cases, the CV of a solution containing all the components, with the exception of NACMP8, was recorded and subtracted from the voltammogram obtained in its presence. The pH of solutions was determined using a Metrohm 605 pH meter calibrated against standard buffer solutions and was adjusted with either HNO<sub>3</sub> or NaOH, as appropriate. All reagents used were of the highest purity available and used as received, unless otherwise indicated. NACMP8 was prepared as previously described.<sup>15</sup>

Sodium azide and sodium bromide were from Riedel de Haën; sodium cyanide, sodium chloride, sodium iodide, pyridine and imidazole were from Merck; 4-cyanopyridine and 4-*N,N*-dimethylaminopyridine were from Aldrich; methoxylamine hydrochloride, hydroxylamine hydrochloride, tetrabutylammonium perchlorate, CAPS and MOPS were from Sigma; ethanolamine, glycine and dry methanol were from BDH; sodium nitrate and sodium thiocyanate were from Saarchem; propylamine was from Fluka. Ethanolamine, pyridine and propylamine were distilled before use.

### 2.2 Equilibrium constants

Equilibrium constants for the co-ordination of weak anionic field ligands, as defined in eqn. 1, were determined by difference spectroscopy methods because they were expected to be small.<sup>21,26</sup>



An increase in ionic strength causes NACMP8 to aggregate;<sup>15</sup> at an ionic strength of 2 mol dm<sup>-3</sup> the species is 80% monomeric, but dimerisation increases markedly at higher ionic strengths. The present investigation was therefore confined to ligand concentrations of ≤ 2 mol dm<sup>-3</sup>.

Equal amounts of NACMP8 were placed in the sample and reference cuvettes in the thermostatted compartment of the spectrophotometer. Aliquots of a ligand solution were injected into the sample cuvette, and similar aliquots of a NaClO<sub>4</sub> solution of the same concentration as the ligand solution were injected into the reference cuvette, thus maintaining the same ionic strength in the two solutions. The inevitable decrease in absorbance that accompanies an increase in ionic strength (11% at the Soret maximum of NACMP8 when the ionic strength reaches 2 mol dm<sup>-3</sup>)<sup>15</sup> was therefore compensated for, such that any changes in absorbance would be a consequence of ligand co-ordination. These absorbance changes were fitted to eqn. 2

$$A = \frac{A_0 + A_1 K [L]}{1 + K [L]} \quad (2)$$

as an objective function with  $A_0$ ,  $A_1$  and  $K$  as variables using standard non-linear least squares methods, where  $A$  is the absorbance at the monitoring wavelength at some concentration of the ligand,  $[L]$ ,  $A_0$  (= 0 in a difference absorbance titration) is the absorbance before any ligand is added, and  $K$  is the equilibrium constant defined in eqn. 1.

### 2.3 Midpoint reduction potentials ( $E_3$ )

Midpoint reduction potentials were determined by CV and are the mean of the potentials of the peak cathodic and anodic waves; they (and all other potentials quoted) are reported relative to the normal hydrogen electrode (NHE). They were determined for the Fe(III)|Fe(II) couple in complexes of NACMP8, His-[FeP]-L (L = H<sub>2</sub>O, OH<sup>-</sup>, Cl<sup>-</sup>, Br<sup>-</sup>, I<sup>-</sup>, SCN<sup>-</sup>, N<sub>3</sub><sup>-</sup>, CN<sup>-</sup>, imidazole, pyridine, 4-cyanopyridine, 4-*N,N*-dimethylaminopyridine, ethanolamine, glycine, propylamine) using solutions with [NACMP8] = 9.89 × 10<sup>-4</sup> mol dm<sup>-3</sup>. Solutions of Cl<sup>-</sup>, Br<sup>-</sup>, I<sup>-</sup>, SCN<sup>-</sup> and N<sub>3</sub><sup>-</sup> were 2 mol dm<sup>-3</sup> in the sodium salt of these anions and the pH was maintained at 7.0 with 0.05 mol dm<sup>-3</sup> MOPS buffer. In the case of the other ligands, the background electrolyte was 0.5 mol dm<sup>-3</sup> NaNO<sub>3</sub>. The concentration of each of these ligands, the pH of the solution, and the buffer used (0.05 mol dm<sup>-3</sup>) was as follows: imidazole (0.025 mol dm<sup>-3</sup>, pH 7.0, MOPS); NaCN (0.05 mol dm<sup>-3</sup>, pH 9.0, CHES); pyridine (0.05 mol dm<sup>-3</sup>, pH 7.0, MOPS); 4-cyanopyridine (0.3 mol dm<sup>-3</sup>, pH 7.0, MOPS); 4-*N,N*-dimethylaminopyridine and ethanolamine (0.05 mol dm<sup>-3</sup>, pH 10.0, CAPS); glycine (0.02 mol dm<sup>-3</sup>, pH 9.8, CAPS); *n*-propylamine (0.1 mol dm<sup>-3</sup>, pH 10.2, CAPS).

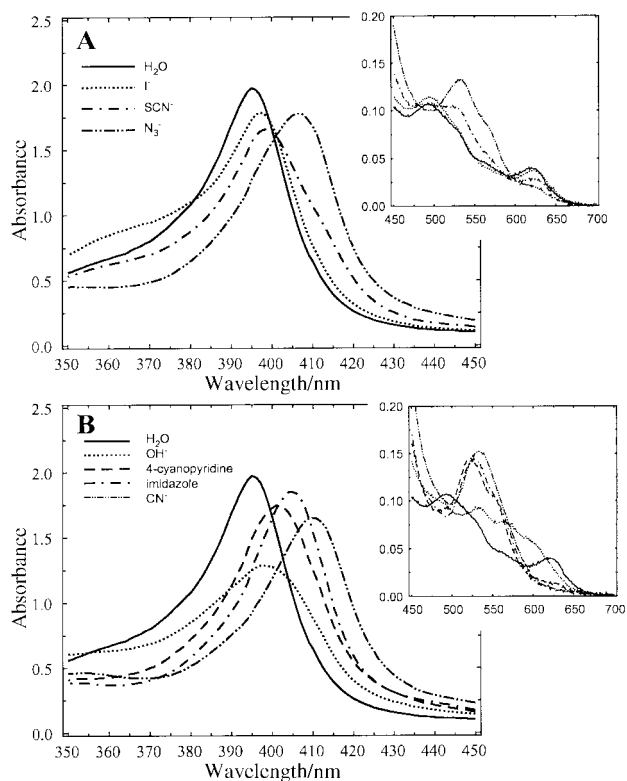


**Fig. 2** UV-visible spectra of complexes of NAcMP8. The spectra for the complexes with  $I^-$ ,  $SCN^-$  and  $N_3^-$  were produced by dissolving NAcMP8 ( $9.48 \times 10^{-6} \text{ mol dm}^{-3}$ ) in  $2 \text{ mol dm}^{-3}$  solutions of their sodium salts in  $50 \text{ mmol dm}^{-3}$  MOPS buffer, pH 7.0, and correspond to 42, 58 and 98% complex formation, respectively. Higher ligand concentrations could not be used because of severe aggregation of NAcMP8 (see text). The  $OH^-$  complex was produced by raising the pH to 10.5 with CAPS buffer. The concentration of 4-cyanopyridine was  $0.3 \text{ mol dm}^{-3}$  (limited by the ligand solubility, and corresponds to 91% complex formation),  $0.025 \text{ mol dm}^{-3}$  for imidazole (>99% complex formation) and  $0.05 \text{ mol dm}^{-3}$  for  $CN^-$  (CHES buffer, pH 9.0, virtually 100% complex formation).

The reduction potential of the imidazole complex of NAcMP8 in 80% (v/v) MeOH and in pure MeOH was determined in the presence of  $0.1 \text{ mol dm}^{-3}$  tetrabutylammonium perchlorate as supporting electrolyte and  $0.05 \text{ mol dm}^{-3}$  MOPS (pH\* 7.0) as buffer.

Molecular orbital calculations were performed using the HYPERCHEM suite of programmes<sup>27</sup> at the UHF/SCF level of theory with an STO-6G\* basis set.

### 3 Results

#### 3.1 The co-ordination of NAcMP8 by weak field ligands

The UV-visible spectra of the complexes studied in this work are shown in Fig. 2. The dependence of the electronic spectra of ferric porphyrins on spin state, and the correlation of such spectra with magnetic properties, is well known.<sup>28,29</sup> Predominantly high spin complexes of Fe(III) porphyrins (actually a mixture of  $S = 3/2$  and  $5/2$  states)<sup>15</sup> are characterised by a Soret (B) band near 397 nm (a composite of transitions to two vibronic components), an N band at 360 nm, the  $Q_v$  [ $a_{1u}, a_{2u}(\pi) \rightarrow e_g^*(\pi^*)$ ] (1,0) vibronic component of the Q-B coupled states at 490 nm,  $Q_o$  at 530 nm, and two charge transfer transitions,  $a_{2u}'(\pi) \rightarrow e_g(d\pi)$  at 570 nm and  $b_{2u}(\pi) \rightarrow e_g(d\pi)$  at 620 nm. The switch from high spin to low spin is accompanied by a red shift of the Soret band to around 410 nm, the  $Q_v$  band to around 530 nm, and the  $Q_o$  band to 560 nm, whilst the N band remains virtually unchanged and the charge transfer transitions move to the near infrared. Species where the ligand induces a spin equilibrium in Fe(III) between  $S = 3/2$ ,  $5/2$  and  $S = 1/2$  states have spectra with features of the two spin states. Thus,

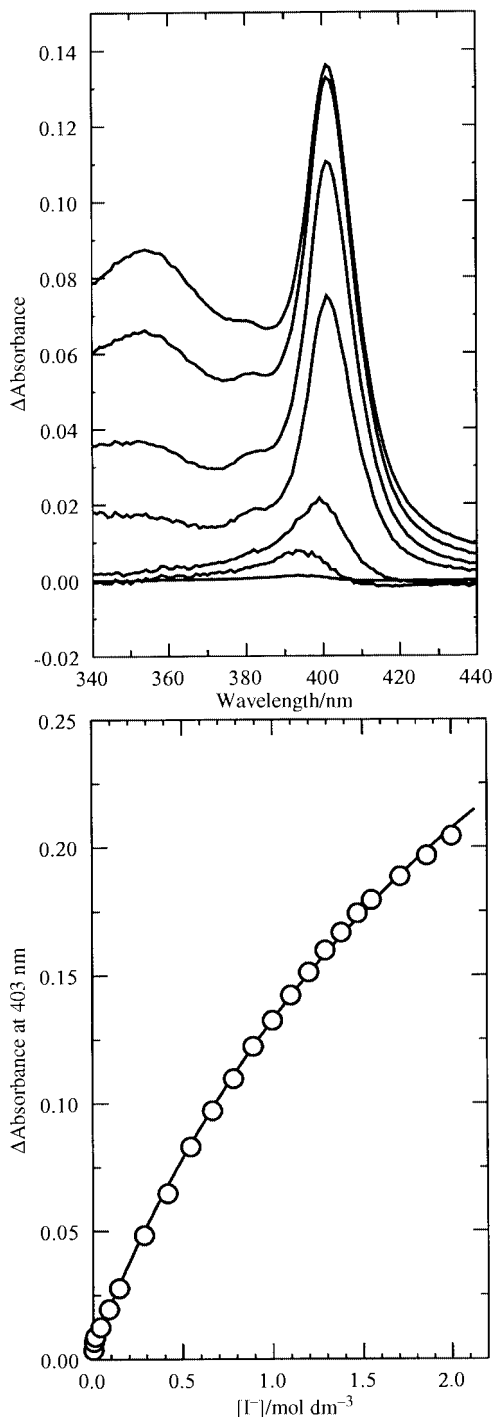


**Fig. 3** Difference titration of NAcMP8 with iodide at 25 °C. The figure on the right shows a fit of the titration data to eqn. 2 in the text.

$H_2O$  and halides co-ordinated to Fe(III) in NAcMP8 produce largely high spin complexes; the complex with  $SCN^-$  is largely high spin, but low spin features are clearly emerging;  $OH^-$  and  $N_3^-$  produce complexes in spin equilibrium; and  $N$ -donor ligands, such as imidazoles and pyridines, and the strong field ligand  $CN^-$ , produce predominantly low spin complexes.

Fig. 3 shows representative difference spectra for the titration of NAcMP8 with  $I^-$  and the fit of the data to eqn. 2. The equilibrium constants for coordination of  $N_3^-$ ,  $SCN^-$ ,  $Cl^-$ ,  $Br^-$  and  $I^-$  are  $25 \pm 3$ ,  $0.69 \pm 0.01$ ,  $0.45 \pm 0.07$ ,  $0.46 \pm 0.04$  and  $0.35 \pm 0.01 \text{ dm}^3 \text{ mol}^{-1}$ , respectively. These results, together with the equilibrium constants for other ligands used in this study and, for comparison, some representative equilibrium constants for co-ordination of these ligands by related haem-peptides, are listed in Table 1 of the supplementary information.†

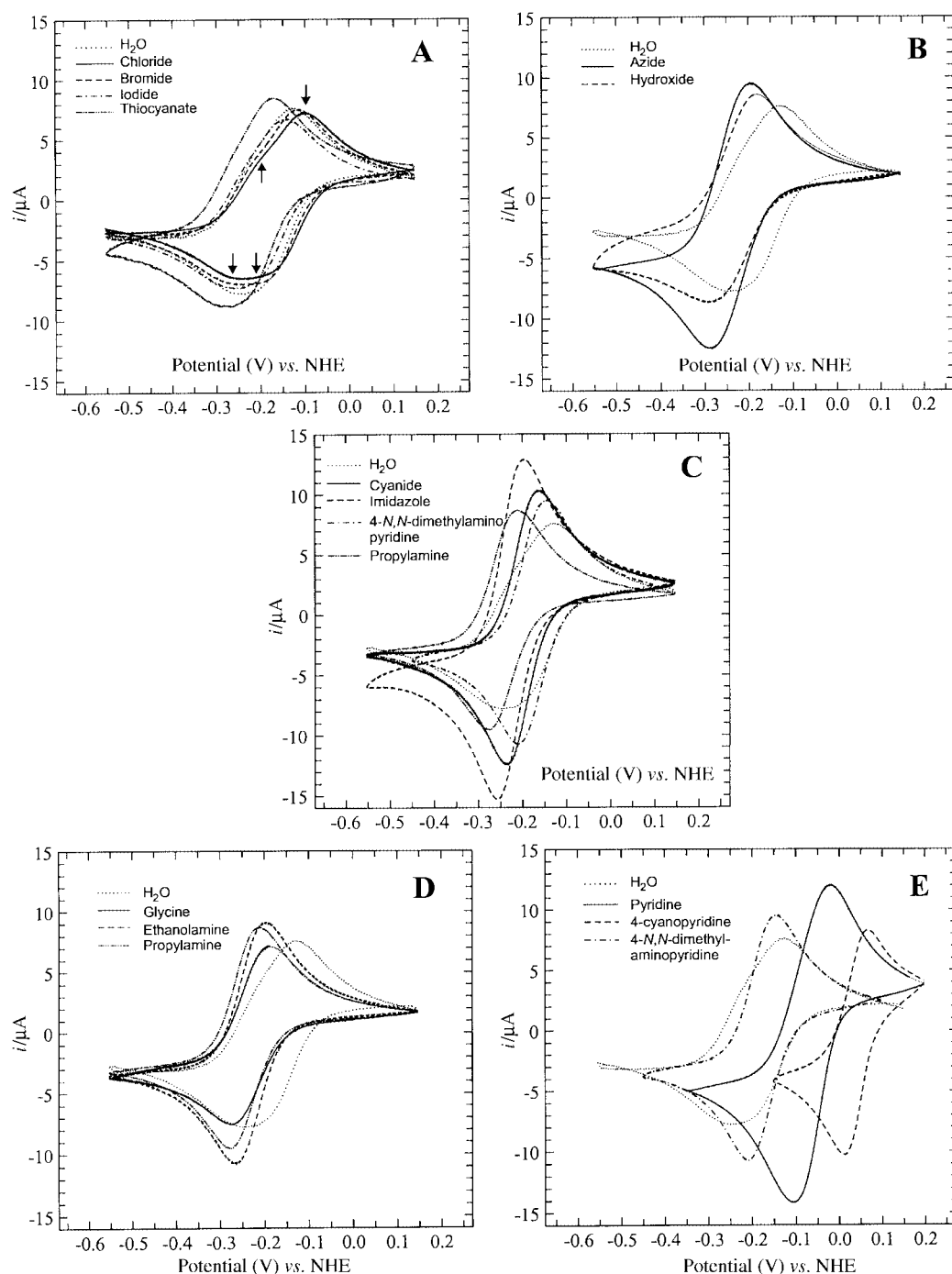


**Fig. 4** Cyclic voltammograms on a glassy carbon electrode of complexes of NAcMP8. A: complexes in which the metal is predominantly high spin; B: complexes with the metal in a spin equilibrium between  $S = 3/2$ ,  $5/2$  and  $S = 1/2$  states; C–E: complexes where the metal is predominantly low spin. For reference, the voltammogram for the aqua complex is reproduced in each figure. The data are rescaled against the standard hydrogen electrode. There are two electrochemically-active species in solutions of high spin complexes (A); this is explicitly shown with arrows for the chloride complex as an example.

### 3.2 The midpoint reduction potential of complexes of NAcMP8

Fig. 4A shows the cyclic voltammograms of the aqua, chloro, bromo, iodo and thiocyanato complexes of NAcMP8. These complexes, in which the metal is predominantly high spin, yield at least two electrochemically-active species; a species which produces a smaller current response is present at more cathodic potentials than the main species. This is indicated, for illustration, on the voltammogram of the chloro complex in Fig. 4A. The potential of this species ( $-0.245$  V) is apparently unchanged by the identity of the axial ligand, whereas that of the principal species decreases in the order  $\text{Cl}^- > \text{Br}^- > \text{H}_2\text{O} > \text{I}^- > \text{SCN}^-$ . Consequently, in the case of the thiocyanato complex—the high spin complex with the

most negative potential examined—the cathodic and anodic waves are only just perceptibly distorted towards negative potentials. By contrast, complexes of NAcMP8 where the metal is either in a spin equilibrium between  $S = 5/2$ ,  $3/2$  and  $S = 1/2$  states (Fig. 4B) or where the metal is low spin (Fig. 4C–E), produce well-defined and symmetrical voltammograms that appear to arise from a single electrochemically-active species. The midpoint reduction potentials are listed in Table 1.

A plot of the log of the peak cathodic current,  $\log i_c^p$ , against the log of the scan rate,  $\log v$ , can be used to determine whether the electrochemical reduction is under diffusion control (slope close to 0.5) or is adsorbed on the electrode (slope close to 1.0).<sup>30</sup> As illustrated in Fig. S1 of the supplementary

**Table 1** Observed midpoint reduction potentials (25 °C vs. NHE) for NAcMP8 with different axial ligands

Axial ligand	$E_2/V$ , vs. NHE <sup>a</sup>	Experimental conditions	Scan rate <sup>b</sup> / mV s <sup>-1</sup>	Peak separation/ mV	$\left(\frac{\log i_c^p}{\log \nu}\right)^c$	$D_0$ ( $\times 10^{-7}$ ) <sup>d</sup> / cm <sup>2</sup> s <sup>-1</sup>	$k_s$ ( $\times 10^{-3}$ ) <sup>d</sup> / cm s <sup>-1</sup>
H <sub>2</sub> O	-0.139(2)	0.5 mol dm <sup>-3</sup> NaNO <sub>3</sub> , pH 7.0 (MOPS)	10 400 <sup>e</sup>	73 83			
H <sub>2</sub> O	-0.134(1)	2.0 mol dm <sup>-3</sup> NaNO <sub>3</sub> , pH 7.0 (MOPS)	10 400 <sup>e</sup>	77 81			
Cl <sup>-</sup>	-0.118(1)	2.0 mol dm <sup>-3</sup> NaCl, pH 7.0 (MOPS)	10 400 <sup>e</sup>	83 92			
Br <sup>-</sup>	-0.131(1)	2.0 mol dm <sup>-3</sup> NaBr, pH 7.0 (MOPS)	10 200 <sup>e</sup>	75 85			
I <sup>-</sup>	-0.159(2)	2.0 mol dm <sup>-3</sup> NaI, pH 7.0 (MOPS)	10 400 <sup>e</sup>	81 87			
SCN <sup>-</sup>	-0.184(1)	2.0 mol dm <sup>-3</sup> NaSCN, pH 7.0 (MOPS)	10 400 <sup>e</sup>	70 77			
OH <sup>-</sup>	-0.204(6)	0.5 mol dm <sup>-3</sup> NaNO <sub>3</sub> , pH 10.5 (CAPS)	10 1000	94 108	0.446(4)	2.35(5)	1.2(6)
N <sub>3</sub> <sup>-</sup>	-0.214(4)	0.5 mol dm <sup>-3</sup> NaN <sub>3</sub> , pH 7.0 (MOPS)	10 1000	93 112	0.448(7)	5.7(2)	2(1)
CN <sup>-</sup>	-0.176(1)	0.05 mol dm <sup>-3</sup> NaCN, pH 7.0 (CHES), $\mu = 0.50$ mol dm <sup>-3</sup> NaNO <sub>3</sub>	10 1000	64 104	0.51(1)	7.1(5)	6(2)
imidazole	-0.203(1)	0.025 mol dm <sup>-3</sup> imidazole, pH 7.0 (MOPS), $\mu = 0.50$ mol dm <sup>-3</sup> NaNO <sub>3</sub>	10 1000	58 83	0.526(5)	11.2(2)	24(14)
imidazole	-0.190(1)	In 80% (v/v) MeOH; 0.025 mol dm <sup>-3</sup> imidazole, pH* 7.0 (MOPS); 0.10 mol dm <sup>-3</sup> Bu <sub>4</sub> NClO <sub>4</sub>	40 1000	63 127	0.40(3)	3.8(6)	4(2)
4-cyanopyridine	+0.062(1)	0.3 mol dm <sup>-3</sup> 4-cyanopyridine, pH 7.0 (MOPS), $\mu = 0.50$ mol dm <sup>-3</sup> NaNO <sub>3</sub>	10 1000	57 81	0.487(8)	4.3(2)	15(13)
pyridine	-0.041(3)	0.05 mol dm <sup>-3</sup> pyridine, pH 7.0 (MOPS), $\mu = 0.50$ mol dm <sup>-3</sup> NaNO <sub>3</sub>	10 1000	76 105	0.498(7)	7.7(3)	3.1(9)
4- <i>N,N</i> -dimethyl-aminopyridine	-0.155(1)	0.05 mol dm <sup>-3</sup> 4- <i>N,N</i> -dimethylamino-pyridine, pH 10.0 (CAPS), $\mu = 0.50$ mol dm <sup>-3</sup> NaNO <sub>3</sub>	10 1000	65 79	0.539(4)	6.1(2)	10.7(3)
ethanolamine	-0.209(3)	0.05 mol dm <sup>-3</sup> ethanolamine, pH 10.0 (CAPS), $\mu = 0.50$ mol dm <sup>-3</sup> NaNO <sub>3</sub>	10 1000	68 97	0.538(4)	6.9(2)	5(2)
glycine	-0.206(1)	0.02 mol dm <sup>-3</sup> ethanolamine, pH 9.8 (CAPS), $\mu = 0.50$ mol dm <sup>-3</sup> NaNO <sub>3</sub>	40 1000	76 126	0.456(7)	1.74(6)	1.2(2)
propylamine	-0.223(2)	0.10 mol dm <sup>-3</sup> propylamine, pH 10.2 (CAPS), $\mu = 0.50$ mol dm <sup>-3</sup> NaNO <sub>3</sub>	10 1000	69 81	0.543(7)	5.9(2)	7(3)

<sup>a</sup> The mean of the potentials of the cathodic and anodic peaks. In the case of ligands where Fe(III) remains predominantly high spin, there is a second electrochemically-active species at more cathodic potentials that overlaps with the predominant species; the midpoint potentials of the latter are listed in this table. The figure in parentheses after each result is the standard deviation of the results over all scan rates examined, and refers to the last significant figure given of the result. <sup>b</sup> Scan rates were varied between 10 and 1000 mV s<sup>-1</sup>. The peak separation is reported only for the extremes of scan rate used. <sup>c</sup> The slope (and standard error) of a plot of the log (peak cathodic current) against log (scan rate). A value close to 0.5 indicates a diffusion-controlled process, whereas a value close to 1 indicates the electrochemically-active species is adsorbed on the electrode (ref. 46). If no value is reported, the overlap of the currents from two electrochemically-active species precludes determination. <sup>d</sup> Numbers in parentheses are standard deviations. <sup>e</sup> Peaks broaden with increasing scan rate; severe overlapping with the second electrochemically-active species precludes obtaining meaningful data at greater scan rates.

information for a representative complex (HIm–NAcMP8)<sup>†</sup> and listed in Table 1, values are all close to 0.5.

For a fully-reversible, diffusion-controlled one-electron reduction, the separation between the cathodic and anodic waves should be 57 mV at 298 K and independent of scan rate.<sup>31</sup> As shown in Table 1, the peak-to-peak potential separations are usually larger than 57 mV, and increase with increasing scan rate; this is characteristic of a quasi-reversible system. The diffusion coefficient,  $D_0$ , in each case was determined from the slope of a plot of the peak cathodic current against the square root of the scan rate<sup>30</sup> and the values are listed in Table 1. Fig. S2 of the supplementary information gives, as an example that obtained for the HIm–NAcMP8 complex.<sup>†</sup> The heterogeneous electron-transfer rate constants were calculated from the scan rate dependence of the difference in peak potentials between the cathodic and anodic waves using Nicholson's method;<sup>31</sup> these values are also listed in Table 1.

Changing the solvent from water to 80% MeOH has virtually no effect on the reduction potential; the diffusion coefficient decreases nearly three fold whilst the rate constant for heterogeneous electron transfer is 6 times smaller.

The diffusion coefficients determined for the various

complexes of NAcMP8 in aqueous solution are in the range 1–11  $\times 10^{-7}$  cm<sup>2</sup> s<sup>-1</sup>; thus, whilst some values are comparable to those reported for a variety of ferric porphyrins in DMF<sup>32</sup> (1.7–2.2  $\times 10^{-6}$  cm<sup>2</sup> s<sup>-1</sup>), others are considerably smaller. The  $D_0$  values are comparable to that for HIm–MP11 in DMSO (1.8  $\times 10^{-7}$  cm<sup>2</sup> s<sup>-1</sup>) at glassy carbon<sup>33</sup> or other<sup>34</sup> electrodes (3.2  $\times 10^{-7}$  cm<sup>2</sup> s<sup>-1</sup>) and for H<sub>2</sub>O–MP11 in aqueous solutions containing surfactant micelles (2.4  $\times 10^{-7}$  cm<sup>2</sup> s<sup>-1</sup>).<sup>22</sup> In 80% MeOH the diffusion coefficient of HIm–NAcMP8 is 3 times smaller than in aqueous solution (3.8  $\times 10^{-7}$  cm<sup>2</sup> s<sup>-1</sup>) (Table 1). This is in agreement with the findings of Mabrouk<sup>33</sup> who reported that the diffusion coefficient of HIm–MP11 is smaller in DMSO than in aqueous solution.

The rate constant for heterogeneous electron transfer varies between 1.2  $\times 10^{-3}$  cm s<sup>-1</sup> for (OH<sup>-</sup>)–NAcMP8 to 2.4  $\times 10^{-2}$  cm s<sup>-1</sup> for HIm–NAcMP8. These results are marginally larger than values reported for H<sub>2</sub>O–MP11 at a glassy carbon electrode (3  $\times 10^{-3}$  cm s<sup>-1</sup>),<sup>19</sup> at a silver electrode (1.29  $\times 10^{-3}$  cm s<sup>-1</sup>),<sup>20,35</sup> and at a surface-modified gold electrode (2  $\times 10^{-3}$  cm s<sup>-1</sup>).<sup>36</sup> The decrease in the  $k_s$  value when changing from aqueous solution to a MeOH–water mixture is a consequence of the lower diffusion coefficient.

## 4 Discussion

### 4.1 The co-ordination of NAcMP8 by weak field ligands

Whilst the co-ordination of strong field ligands by the haempeptides has been extensively studied<sup>16,21,37–44</sup> (representative data are listed in Table S1 of the supplementary information),† much less attention has been paid to weaker field ligands. We find that the affinity of Fe(III) for Cl<sup>−</sup>, Br<sup>−</sup>, I<sup>−</sup> and SCN<sup>−</sup> is very low (*i.e.*  $\log K < 1$ ). The electronic spectra (Fig. 2) show that Fe(III) remains predominantly high spin. For N<sub>3</sub><sup>−</sup> which causes the metal to enter an  $S = 3/2, 5/2 \longleftrightarrow S = 1/2$  equilibrium,  $\log K$  increases to 1.4. Binding constants are orders of magnitude larger for ligands that produce a predominantly low spin complex (primary amines, pyridines, imidazoles, cyanide; Table S1).† There thus appears to be a simple relationship between the ligand field stabilisation energy elicited from the metal ion, and the magnitude of  $\log K$ . However, within any class of ligands other factors are important. For example, there is a linear relationship between the donor power of *N*-donor ligands (as determined by their p*K*<sub>a</sub> values) and  $\log K$ ;<sup>16,40,42,45</sup> metal–ligand  $\pi$  bonding is a contributing factor<sup>16</sup> and the secondary interactions between non-co-ordinating substituents on the ligand and haem or peptide chain functional groups will influence the magnitude of  $\log K$ .<sup>16</sup>

### 4.2 The reduction potentials of high spin complexes of NAcMP8

The study of the reduction potential of NAcMP8 with weak field ligands is complicated by their low binding constants, the increase in aggregation of NAcMP8 on increasing ionic strength,<sup>15</sup> and the precipitation of the haempeptide from solution at ionic strength  $> ca. 2.5 \text{ mol dm}^{-3}$ . Although NAcMP8 is much less prone to aggregation than MP8 itself (the blocking of the *N*-terminus by acetylation precludes the formation of a low spin dimer in which this amino group co-ordinates Fe(III) intermolecularly) the compound does still aggregate, probably through  $\pi$ – $\pi$  interactions; this may be approximated as a dimerisation with an equilibrium constant  $K_D = 1.09 \times 10^4 \text{ dm}^3 \text{ mol}^{-1}$ .<sup>15</sup> To obtain a sufficiently large electrode current in a CV study requires a haempeptide concentration in the millimolar range; at a concentration of  $9.89 \times 10^{-4} \text{ mol dm}^{-3}$ , as used in this study, NAcMP11 is only 19% monomeric. The aggregation persists with weak field ligands such as chloride<sup>46</sup> but not with strong field ligands such as imidazole,<sup>46a</sup> cyanide or ethanolamine,<sup>46b</sup> where the haempeptide is strictly monomeric at least up to a concentration of  $2 \text{ mmol dm}^{-3}$ . However, previous work on haempeptides (see Introduction) suggests that the reduction potential is relatively insensitive to aggregation.

The insolubility of the haempeptide in solutions of high ionic strength limited the present study to a Cl<sup>−</sup>, Br<sup>−</sup>, I<sup>−</sup> and SCN<sup>−</sup> concentration of  $\leq 2.00 \text{ mol dm}^{-3}$ . Using the binding constants measured (see Results), the extent of formation of the chloro, bromo, iodo and thiocyanato complexes is 47, 48, 42 and 58%, respectively, so that the cyclic voltammograms of Fig. 4A arise from a mixture of the aqua and the halo or thiocyanato complexes of NAcMP8; the  $E_{1/2}$  values for these complexes listed in Table 1 must be treated as only approximate.

The nature of the common species that is reduced at a more negative potential than the major species in solutions of high spin complexes of NAcMP8 is unclear. It is not the aqua complex of NAcMP8, as the species is also present in a solution of H<sub>2</sub>O–NAcMP8. Since the affinity of the metal ion for weak field ligands is low, we tentatively suggest that it is a species adsorbed onto the electrode surface, possibly with functionalities such as carboxylate groups on the glassy carbon electrode surface providing the axial ligand for the metal ion. The close overlap with the peaks for the main species precludes meaningful measurement of the peak cathodic current; had this been possible, this conclusion could have been tested by exam-

ining the relationship between  $\log(i_p^c)$  and  $\log v$  which, for an adsorbed species, should give a slope close to unity. Razumas and co-workers<sup>20,35</sup> observed a similar species on a silver electrode when working with solutions of MP11. In their case, the peak separation between the adsorbed species and the main species (the histidine complex of MP11) allowed for meaningful determination of peak currents.

### 4.3 Reduction potentials and spin state

A number of low spin complexes (L = imidazole, ethanolamine, glycine, propylamine, cyanide) have remarkably similar reduction potentials that span less than 50 mV ( $E_{1/2} = -0.203 \pm 0.015 \text{ V}$ ); however, the low spin complexes where L = pyridine or one of its derivatives have substantially more positive reduction potentials. The average reduction potential of the complexes in spin equilibrium (L = OH<sup>−</sup>, N<sub>3</sub><sup>−</sup>),  $E_{1/2} = -0.209 \pm 0.005 \text{ V}$ , is not statistically different from the majority of the low spin complexes. High spin complexes have somewhat more positive reduction potentials ( $E_{1/2} = -0.146 \pm 0.023 \text{ V}$ ). There is therefore no strong correlation between  $E_{1/2}$  and the spin state of the metal ion in haempeptide complexes. A similar observation on Fe(TPP) complexes has been made.<sup>47</sup>

### 4.4 Reduction potentials and the hardness of the axial ligand

For high spin complexes of L–NAcMP8, the reduction potential decreases in the order L = Cl<sup>−</sup> > Br<sup>−</sup> > H<sub>2</sub>O > I<sup>−</sup> > SCN<sup>−</sup>. Insofar as the halides are concerned, this parallels the hardness,  $\eta$ , of the anion (half the difference between the ionisation energy and the electron affinity),<sup>48</sup> deduced, as discussed by Pearson, from the experimental values of the free atoms, since hardness is independent of charge (although it varies inversely with radius). Thus, the ferric state becomes more stable as the softness of the axial ligand increases, presumably as a consequence of the increasing ability of the ligand to transfer electron density to the metal centre.

Whilst a factor, the hardness parameter is insufficient to explain the observed trends. Water ( $\eta = 9.5$ ) is significantly harder than Cl<sup>−</sup> ( $\eta = 4.7$ ),<sup>48</sup> yet H<sub>2</sub>O–NAcMP8 has a more negative potential than Cl–NAcMP8. The hardness of SCN<sup>−</sup> is unknown, but can be estimated using Pearson's procedure. Using an STO-6G\* basis set, a model of the SCN radical was geometry-optimised using an UHF/SCF procedure, and the energies of the HOMO and LUMO were determined. This was also done for atomic Cl, Br, I, and the OH and CN radicals. From Koopman's theorem, the ionisation energy,  $I = -E_{\text{HOMO}}$ , and the electron affinity,  $A = E_{\text{LUMO}}$ ; hence  $\eta = (I - A)/2$ . Values of  $\eta$  from this approach and with this basis set are substantially larger than the experimental values (for example,  $\eta$  for CN<sup>−</sup> and Cl<sup>−</sup> are 8.14 and 6.65, respectively, whereas the experimental values<sup>48</sup> are 5.1 and 4.7, respectively). Nevertheless, there is a good linear correlation ( $R^2 = 0.97$ ) between the *ab initio* and the experimental values. From this correlation we can estimate  $\eta_{\text{SCN}^-} = 0.56$ . SCN<sup>−</sup> is predicted to be harder than I<sup>−</sup> ( $\eta = 3.70$ ), but the reduction potential of the SCN–NAcMP8 (−0.184 V) is more negative than that of the iodo complex (−0.159 V). It is unknown whether the thiocyanato ligand is *S*- or *N*-bonded in SCN–NAcMP8. Precedents in porphyrin chemistry suggest an *N*-bound species, as in Fe(OEP)(py)(NCS) and in Fe(TPP)(py)(NCS).<sup>49</sup> Since S is harder than I, and the local hardness of N will be larger than that of S, considerations of linkage isomerism do not resolve the issue.

Examples of the stabilisation of Fe(II) relative to Fe(III) as the softness of the axial ligand increases are known. The bis-(histidine) complex of Fe-mesoporphyrin has a potential of −0.220 V; the combination of His and Met as axial ligands gives a potential of −0.110 V; but with two methionines as axial ligands, the potential is 0.020 V.<sup>50</sup> A similar effect is seen in the early work of Harbury and co-workers on MP8.<sup>51–53</sup> The reduction potential of L = imidazole (*N*-donor; −0.210 V,

cf.  $-0.203$  V reported here for HIm–NACMP8) increases to  $-0.050$  V when L = acetylmethionine (*S*-donor). However, we note that substitution of H<sub>2</sub>O by pyridine in NACMP8 causes the reduction potential to increase by nearly 100 mV (Table 1); but when pyridine displaces both water molecules in FePPIX, the reduction potential increases by an insignificant 5 mV.<sup>54</sup>

#### 4.5 Reduction potentials and ligand basicity

The reduction potentials of NACMP8 complexes with pyridines and primary amines parallel the  $pK_a$  values of the ligands (the potentials increase in the order L = 4-cyanopyridine < pyridine < 4-*N,N*-dimethylaminopyridine, and ethanolamine  $\approx$  glycine < propylamine); an increase in ligand basicity stabilises the Fe(III) state relative to the Fe(II) state. This effect has been observed by Walker and co-workers<sup>55</sup> in an investigation of the reduction of bis(pyridine) complexes of [Fe{(2,6-F<sub>2</sub>)-TPP}(L)<sub>2</sub>] in DMF. Kadish and co-workers<sup>56,57</sup> also reported a direct correlation between the basicity of a co-ordinated pyridine and the potential of the Fe(III)|Fe(II) couple in bis(pyridine) adducts of Fe(III)TPP.

#### 4.6 Reduction potentials and the haem environment

The haem environment may have an effect on the reduction potential of an iron porphyrin. Mabrouk<sup>33</sup> has shown that the reduction potential of HIm–MP11 in DMSO is  $-0.074$  V, significantly more positive than reduction potentials of  $-0.203$  V reported here for HIm–NACMP8,  $-0.200$  V for HIm–MP11<sup>33</sup> and  $-0.190$  V for HIm–MP8 (at pH 7.0),<sup>47</sup> all in aqueous solution. Thus, a non-aqueous environment usually stabilises Fe(II) relative to Fe(III) in the haempeptides, and in other metalloporphyrins,<sup>47,55–58</sup> but exceptions have been reported.<sup>58</sup> This is consistent with the charge distribution near the metal centre; the +2 charge on the metal in the ferrous complex is neutralised by the  $-2$  charge of the porphyrin dianion so that the ferrous state becomes more stable relative to the ferric state as the dielectric constant of the medium decreases. We found that in 80% MeOH the reduction potential of HIm–NACMP8 is not significantly different from that in aqueous solution. The reduction in pure MeOH is irreversible; the position of the peak cathodic wave was strongly dependent on the scan rate, broadening as it decreased from  $-0.263$  to  $-0.374$  V when the scan rate was increased from 10 to 1000 mV s<sup>-1</sup>, respectively. If we assume a peak separation between the observed cathodic wave and the putative anodic wave of between 60 and 150 mV (see Table 1), then the reduction potential in pure MeOH is probably not significantly different to that in aqueous solution or in MeOH–H<sub>2</sub>O mixtures.

#### 4.7 Rate constants for heterogeneous electron transfer

There is no obvious correlation between the rate constant for heterogeneous electron transfer,  $k_s$ , and the reduction potential of L–NACMP8. On average, compounds containing an anionic ligand have  $k_s$  values (where these could be determined) marginally smaller than those with a neutral ligand ( $3 \pm 2 \times 10^{-4}$  and  $9 \pm 7 \times 10^{-4}$  cm s<sup>-1</sup>, respectively). If this is significant, it presumably reflects an electrostatic effect where NACMP8 species with a neutral axial ligand have a residual positive charge at the metal centre, whilst those carrying an anionic ligand are neutral. It is generally accepted that the pathway of electron transfer to the metal in a metalloporphyrin proceeds through the porphyrin ring itself, rather than through the axial ligands,<sup>59</sup> and this would explain the relative insensitivity of  $k_s$  values to the nature of the axial ligand. This is in agreement with both the self-exchange rate constant for the haempeptides<sup>24</sup> and their chemical reduction by dithionite,<sup>25</sup> for which the rate constants are insensitive to the nature of the axial ligand.

#### 4.8 Conclusions

The factors controlling the reduction potential of a metalloprotein have been explored for many years. Perhaps the classic example is the cytochrome *c* family of proteins, the reduction potentials of which span some 0.75 V (pH 7), from +0.358 V for cyt *c*<sub>2</sub> from *Rhodobacter capsulatus*<sup>60</sup> to  $-0.375$  V for one of the haem groups of cyt *c*<sub>3</sub> from *Desulfovibrio vulgaris*,<sup>61</sup> whilst free protohaem (aqueous solution, pH 7) has a potential of  $-0.115$  V.<sup>59</sup> The co-ordination of Fe by His/Met is associated with redox potentials in the +0.4 to 0 V range; co-ordination by the harder ligand combination His/His leads to a potential in the 0 to  $-0.4$  V range.<sup>62</sup> Site-directed mutagenesis studies elegantly illustrate the influence of the axial ligand field. Replacement of His/His with His/Met in *D. vulgaris* cyt *c*' leads to an increase in redox potential of 0.15 V;<sup>63,64</sup> replacement of Met-80 in cyt *c* by His or Leu (leading to the axial ligand combinations His/His and H<sub>2</sub>O/His, respectively, leads to a decrease in the reduction potential by some 0.2 V.<sup>65</sup> But such clear-cut effects are not always observed, thus, replacement of the proximal His-18 with Arg in yeast iso-2-cyt *c* leads to no significant change in redox potential.<sup>66</sup>

Clearly the inner co-ordination sphere of the metal plays a role in controlling the reduction potential, but the realisation that proteins with the same metal centre, containing the same ligands, can have very different reduction potentials indicates the importance of other factors, amongst these the charges and dipoles of surrounding amino acids, the solvent accessibility to the metal-binding cavity, and the non-polar nature of the protein matrix.<sup>67,68</sup> The present work, in which we vary a single axial ligand of an iron porphyrin, emphasises that changing the axial ligand field can modulate the reduction potential only by a relatively small amount. This is in agreement with a recent report<sup>69</sup> on density functional (B3LYP) calculations on realistic models for the metal centres of a variety of blue copper proteins, in which it is shown that variation of the ligands of the metal ion can account for at most a variation in reduction potential of some 140 mV, a fraction of the 800 mV observed in nature.

#### Acknowledgements

The financial assistance of the National Research Foundation and the University of the Witwatersrand is gratefully acknowledged. The Carnegie Mellon Foundation is thanked for a postgraduate fellowship to P. R. V.

#### References

- 1 D. A. Baldwin, H. M. Marques and J. M. Pratt, *J. Inorg. Biochem.*, 1986, **27**, 245.
- 2 D. W. Low, H. B. Gray and J. O. Duus, *J. Am. Chem. Soc.*, 1997, **119**, 1.
- 3 P. A. Adams, D. A. Baldwin, H. M. Marques, in *Cytochrome c: A Multidisciplinary Approach*, ed. R. A. Scott and A. G. Mauk, University Science, Mill Valley, CA, 1996, pp. 635–692.
- 4 H. M. Marques, M. S. Shongwe, O. Q. Munro and T. J. Egan, *S. Afr. J. Chem.*, 1997, **50**, 166.
- 5 J. Aron, D. A. Baldwin, H. M. Marques, J. M. Pratt and P. A. Adams, *J. Inorg. Biochem.*, 1986, **27**, 227.
- 6 D. A. Baldwin, H. M. Marques and J. M. Pratt, *FEBS Lett.*, 1985, **183**, 309.
- 7 D. A. Baldwin, H. M. Marques and J. M. Pratt, *J. Inorg. Biochem.*, 1987, **30**, 203.
- 8 I. D. Cunningham, J. L. Bachelor and J. M. Pratt, *J. Chem. Soc., Perkin Trans. 2*, 1994, 1347.
- 9 P. A. Adams and C. Adams, *J. Inorg. Biochem.*, 1988, **34**, 177.
- 10 P. A. Adams and R. D. Goold, *J. Chem. Soc., Chem. Commun.*, 1990, 97.
- 11 P. A. Adams, *J. Chem. Soc., Perkin Trans. 2*, 1990, 1407.
- 12 A. M. Osman, J. Koerts, M. G. Boersma, S. Boeren, C. Veeger and I. M. C. M. Rietjens, *Eur. J. Biochem.*, 1996, **240**, 232.
- 13 D. W. Urry and J. W. Pettegrew, *J. Am. Chem. Soc.*, 1967, **89**, 5276.

- 14 O. Q. Munro, M. de Wet, H. Pollak, J. van Wyk and H. M. Marques, *J. Chem. Soc., Faraday Trans.*, 1998, **94**, 1743.
- 15 O. Q. Munro and H. M. Marques, *Inorg. Chem.*, 1996, **35**, 3752.
- 16 H. M. Marques, O. Q. Munro, T. Munro, M. de Wet and P. R. Vashi, *Inorg. Chem.*, 1999, **38**, 2312.
- 17 H. M. Marques, D. A. Baldwin and J. M. Pratt, *J. Inorg. Biochem.*, 1987, **29**, 77.
- 18 H. M. Marques and A. Rousseau, *Inorg. Chim. Acta*, 1996, **248**, 115.
- 19 R. Santucci, H. Reinhard and M. Brunori, *J. Am. Chem. Soc.*, 1988, **110**, 8536.
- 20 V. J. Razumas, A. V. Gundavičius, J. D. Kazlauskaitė and J. J. Kulys, *J. Electroanal. Chem.*, 1989, **271**, 155.
- 21 H. M. Marques and C. B. Perry, *J. Inorg. Biochem.*, 1999, **75**, 281.
- 22 D. K. Das and O. K. Medhi, *J. Chem. Soc., Dalton Trans.*, 1998, 1693.
- 23 S. A. Kazmi, M. A. Mills, Z. W. Pitluk and R. A. Scott, *J. Inorg. Biochem.*, 1985, **24**, 9.
- 24 J. Peterson and M. T. Wilson, *Inorg. Chim. Acta*, 1987, **135**, 101.
- 25 G. McLendon and M. Smith, *Inorg. Chem.*, 1982, **21**, 847.
- 26 Y. Huang and R. J. Kassner, *J. Biol. Chem.*, 1981, **259**, 10309.
- 27 HYPERCHEM, Computational Chemistry Programs, Hypercube, Inc., Gainesville, FL, 1996.
- 28 M. W. Makinen and A. K. Churg, in *Iron Porphyrins, Part 1*, ed. A. B. P. Lever and H. B. Gray, Physical Bioinorganic Chemistry Series, Addison-Wesley, Reading, MA, 1983, p. 141.
- 29 W. A. Eaton and J. Hofrichter, *Methods Enzymol.*, 1981, **76**, 175.
- 30 D. K. Gosser, *Cyclic Voltammetry: Simulation and Analysis of Reaction Mechanisms*, VCH, New York, 1993, p. 43.
- 31 R. S. Nicholson, *Anal. Chem.*, 1965, **37**, 1351.
- 32 K. M. Kadish and G. Larson, *Bioinorg. Chem.*, 1977, **7**, 95.
- 33 P. A. Mabrouk, *Anal. Chim. Acta*, 1995, **307**, 245.
- 34 P. A. Mabrouk, *Anal. Chem.*, 1996, **68**, 189.
- 35 V. Razumas, J. Kazlauskaitė, T. Ruzgas and J. Kulys, *Bioelectrochem. Bioenerg.*, 1992, **28**, 159.
- 36 V. Razumas and T. Arnebrant, *J. Electroanal. Chem.*, 1997, **427**, 1.
- 37 M. T. Wilson, R. J. Ranson, P. Masiakowski, E. Czarnecka and M. Brunori, *Eur. J. Biochem.*, 1977, **77**, 193.
- 38 D. C. Blumenthal and R. J. Kassner, *J. Biol. Chem.*, 1980, **255**, 5859.
- 39 M. M. M. Saleem and M. T. Wilson, *Inorg. Chim. Acta*, 1988, **153**, 93.
- 40 M. S. A. Hamza and J. M. Pratt, *J. Chem. Soc., Dalton Trans.*, 1993, 1647.
- 41 H. M. Marques, M. P. Byfield and J. M. Pratt, *J. Chem. Soc., Dalton Trans.*, 1993, 1633.
- 42 M. P. Byfield, M. S. A. Hamza and J. M. Pratt, *J. Chem. Soc., Dalton Trans.*, 1993, 1641.
- 43 T. Shimizu, T. Nozawa and M. Hatano, *J. Biochem. (Tokyo)*, 1982, **91**, 1951.
- 44 A. J. M. Sadeque, T. Shimizu and M. Hatano, *Inorg. Chim. Acta*, 1987, **135**, 109.
- 45 M. S. A. Hamza and J. M. Pratt, *J. Chem. Soc., Dalton Trans.*, 1994, 1367.
- 46 (a) H. M. Marques, *Inorg. Chem.*, 1990, **29**, 1597; (b) H. M. Marques, unpublished observations.
- 47 L. A. Bottomley and K. M. Kadish, *Inorg. Chem.*, 1981, **20**, 1348.
- 48 R. G. Pearson, *Inorg. Chem.*, 1988, **27**, 734.
- 49 W. R. Scheidt, Y. J. Lee, D. K. Geiger, K. Taylor and K. Hatano, *J. Am. Chem. Soc.*, 1982, **104**, 3367.
- 50 P. K. Warne and L. P. Hager, *Biochemistry*, 1970, **9**, 1606.
- 51 H. A. Harbury and P. A. Loach, *J. Biol. Chem.*, 1960, **235**, 3646.
- 52 H. A. Harbury, J. R. Cronin, M. W. Fanger, T. P. Hettlinger, A. J. Murphy, Y. P. Meyer and S. N. Vinogradov, *Proc. Natl. Acad. Sci. U. S. A.*, 1965, **54**, 1658.
- 53 H. A. Harbury and P. A. Loach, *J. Biol. Chem.*, 1960, **235**, 3640.
- 54 J. Shack and W. M. Clark, *J. Biol. Chem.*, 1947, **171**, 143.
- 55 M. J. M. Nasset, N. V. Shokhirev, P. D. Enemark, S. E. Jacobson and F. A. Walker, *Inorg. Chem.*, 1996, **35**, 5188.
- 56 S. I. Kelly and K. M. Kadish, *Inorg. Chem.*, 1982, **21**, 3631.
- 57 K. M. Kadish and L. A. Bottomley, *Inorg. Chem.*, 1980, **19**, 832.
- 58 R. J. Kassner, *Proc. Natl. Acad. Sci. U. S. A.*, 1972, **69**, 2263.
- 59 G. R. Moore and G. W. Pettigrew, *Cytochrome c: Evolutionary, Structural and Physicochemical Aspects*, Springer, Berlin, 1990.
- 60 M. M. Benning, G. Wesenberg, M. S. Caffrey, R. G. Bartsh, T. E. Meyer, M. A. Cusanovich, I. Rayment and M. Holden, *J. Mol. Biol.*, 1991, **220**, 673.
- 61 Y. Morimoto, T. Tani, H. Okumura, Y. Higuchi and N. Yasuoka, *J. Biochem. (Tokyo)*, 1991, **110**, 532.
- 62 A. Dolla, L. Blanchard, F. Guerlesquin and M. Bruschi, *Biochimie*, 1994, **76**, 471.
- 63 I. Mus-Veteau, A. Dolla, F. Guerlesquin, F. Payan, M. Czizek, R. Haser, P. Biancot, J. Haladjian, B. Rapp-Giles, J. Wall, G. Voordouw and M. Bruschi, *J. Biol. Chem.*, 1992, **267**, 16851.
- 64 A. Dolla, L. Florena, P. Bianco, P. Haladjian, G. Voordouw, E. Forest, J. Wall, F. Guerlesquin and M. Bruschi, *J. Biol. Chem.*, 1994, **269**, 6340.
- 65 A. L. Raphael and H. B. Gray, *J. Am. Chem. Soc.*, 1991, **113**, 1038.
- 66 T. N. Sorrel and P. Martin, *J. Am. Chem. Soc.*, 1989, **111**, 766.
- 67 A. K. Churg and A. Warshel, *Biochemistry*, 1986, **25**, 1675.
- 68 A. G. Mauk and G. R. Moore, *J. Biol. Inorg. Chem.*, 1997, **2**, 119.
- 69 M. H. M. Olsson and R. Ryde, *J. Biol. Inorg. Chem.*, 1999, **4**, 654.